

A Wide-Angle and Wide-Band Circular Polarizer Using a Bi-Layer Metasurface

Bao-Qin Lin*, Jianxin Guo, Yanwen Wang, Zuliang Wang,
Baigang Huang, and Xiangwen Liu

Abstract—In this work, a wide-angle and wide-band transmission-type circular polarizer based on a bi-layer anisotropic metasurface is proposed, in which the unit cell consists of two layers of identical patterned metal films deposited on the two sides of a homogeneous dielectric layer, and the geometric pattern of the metal film is a square aperture surrounding a concentric square-corner-truncated square patch. The simulated results show that the polarizer can realize a linear-to-circular polarization conversion at both x - and y -polarized incidences in the frequency range from 7.63 to 11.13 GHz with a relative bandwidth of 37.3%, and it can maintain a stable polarization conversion performance under large-range incidence angles. Moreover, it has no asymmetric transmission effect, and the transmission coefficients at x - and y -polarized incidences are completely equal. Finally, one experiment is carried out, and the simulated and measured results are almost in agreement with each other.

1. INTRODUCTION

Circularly polarized (CP) waves play an important role in various wireless systems including mobile communications, radar tracking, satellite communications and navigation systems, which are preferred due to the advantages such as simplifying alignment and overcoming Faraday rotation [1]. To generate a CP wave, in addition to the way to generate it directly using CP antenna, an alternative effective way is to generate a linearly polarized (LP) wave and employ a CP polarizer to convert it into a CP wave, and this way is particularly attractive in situations where the radiating system is a planar antenna array, and generating CP waves at the each element is not convenient. Moreover, one already designed LP antenna can be modified as a CP one by using a proper CP polarizer. However, for this, one of the challenging issues is to design a proper CP polarizer.

Polarizer is a kind of polarization control device which is used to convert an incident wave with a given polarization to a reflected or transmitted wave with a different polarization, and it can be realized in different ways. Conventional polarization converters were usually designed by using the birefringence effect and optical activity of natural materials, which usually suffer from bulky volumes, high losses, and narrow bandwidth in practical applications [2, 3]. Over the past decade, it has been found that metamaterials (MMs) can provide a convenient way to control the polarization state of an EM wave. Based on various MMs, many different polarization converters have been proposed [4–34], and they were usually realized in one of the following two methods: one is to divide a LP wave into two orthogonal components and generate a different phase between them (the fundamental of birefringence effect) by using anisotropic MMs, and the other is to mimic molecule chirality (the fundamental of optical activity) by using chiral MMs. The existing literature indicates that anisotropic two-dimensional MMs (also called metasurfaces) are more suitable for the design of reflective polarizers, and now a number of high-efficiency and ultra-wideband reflective linear polarizers were achieved by using multiple

Received 9 January 2018, Accepted 18 April 2018, Scheduled 2 May 2018

* Corresponding author: Bao-Qin Lin (aflbq@sina.com).

The authors are with the School of Information Engineering, Xijing University, Xi'an, China.

plasmon resonances of different anisotropic metasurfaces [4–14]. However, chiral MMs are convenient for designing transmissive polarizers. Based on various chiral MMs, most transmissive polarizers, which can realize linear [15–23] or circular [24–35] polarization conversion, have been proposed. In addition, because of the asymmetry of these chiral MM structures, in most cases, the asymmetric transmission effect, which means that the transmission coefficients are different at the incidences with different polarizations (x/y - or RHCP/LHCP-polarizations), can also be observed at the same time [17–23, 25–35]. The asymmetric transmission effect can be used for polarization selection; however, it should be avoided sometimes to ensure that the transmission coefficients are the same at the incidences with different polarizations.

In this work, we propose a novel bi-layer anisotropic metasurface, which can be used as a transmission-type CP polarizer and realize wide-angle and wide-band LP-to-CP polarization conversion at both x - and y -polarized incidences. Moreover, the metasurface is an orthotropic structure with a pair of mutually perpendicular symmetric axes u and v along $\pm 45^\circ$ directions with respect to the y -axis, and its transmission coefficients at x - and y -polarized incidences are completely equal.

2. DESIGN AND ANALYSIS

The unit cell of the proposed metasurface is shown in Fig. 1. It consists of two layers of patterned metal films deposited on the two sides of a homogeneous dielectric layer. The geometric patterns of the two layers of metal films are completely the same, which is just a large square aperture surrounding a concentric square-corner-truncated square patch, and the geometrical parameters are shown in Fig. 1. After optimal selection, these geometrical parameters are chosen as follows: $P = 8.0$ mm, $l = 7.6$ mm, $w = 4.9$ mm, $c = 2.1$ mm and $d = 2.4$ mm. In addition, the dielectric layer is with a dielectric constant $\epsilon_r = 1.8$ and a loss tangent $\tan \delta = 0.001$.

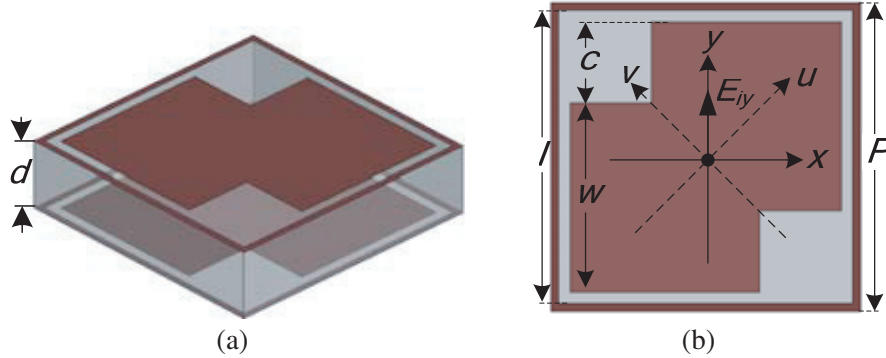


Figure 1. Unit cell of the proposed metasurface: (a) 3D view; (b) Top view.

To numerically analyze the performance of our design, we suppose that the metasurface is located in the X - Y plane, and one y -polarized wave $E^i = E_0 e^{-jkz} \hat{e}_y$ is normally incident on it. For the polarizer is an orthotropic structure, the reflected and transmitted waves would consist of both x - and y -polarized components. Now we define the reflection/transmission coefficients as $r_{mn} = E_m^r/E_n^i/t_{mn} = E_m^t/E_n^i$, wherein the first and second subscripts m and n correspond to the polarized components of the reflected/transmitted and incident fields, respectively. With the simulation using Ansoft HFSS, the magnitudes of the reflection and transmission coefficients, together with the phase difference between the cross- and co-polarization transmission coefficients $\Delta\varphi_{yx} = \arg(t_{yy}) - \arg(t_{xy})$, are obtained and shown in Fig. 2. In Fig. 2(a), it is indicated that the metasurface has a band-pass response, and the center frequency of the pass-band is located at 10.73 GHz, wherein the magnitudes of r_{xy} and r_{yy} are both close to zero, and the amplitudes of t_{xy} and t_{yy} are both close to 0.7. In addition, Fig. 2(b) shows that the phase difference $\Delta\varphi_{yx}$ is much close to -90° at the center frequency 10.73 GHz, and it is implied that the total transmitted wave has been converted to an RHCP one for it travels in the $+z$ direction.

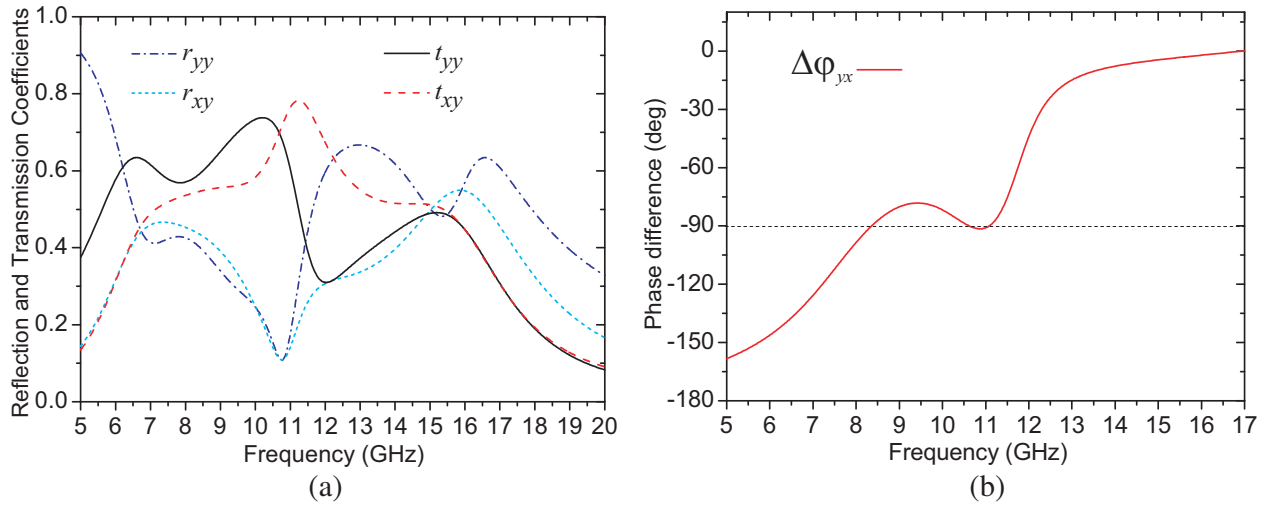


Figure 2. Simulated results of the metasurface at y -polarized normal incidence: (a) The magnitudes of r_{xy} , r_{yy} , t_{xy} and t_{yy} ; (b) The phase difference $\Delta\varphi_{yx}$.

In fact, the transmitted wave is still an elliptically polarized wave. To evaluate the polarization conversion performances of the proposed metasurface in a certain frequency range, we calculate the axial ratio (AR) of the transmitted wave by using the following formula:

$$AR = \left(\frac{|t_{yy}|^2 + |t_{xy}|^2 + \sqrt{a}}{|t_{yy}|^2 + |t_{xy}|^2 - \sqrt{a}} \right)^{1/2}, \quad (1)$$

wherein $a = |t_{yy}|^4 + |t_{xy}|^4 + 2|t_{yy}|^2|t_{xy}|^2 \cos(2\Delta\varphi_{yx})$. The calculated results, shown in Fig. 3, indicate that the AR is lower than 3 dB in the frequency range from 7.63 to 11.13 GHz, wherein the transmitted wave can be considered as a CP one, thus the metasurface can be used as a CP polarizer in this frequency band, which is corresponding to a 37.3% fractional bandwidth. In addition, Fig. 3 shows the total transmittance $T_{all} = |t_{yy}|^2 + |t_{xy}|^2$ at the same time, and it is indicated that the insertion loss of the CP polarizer can be kept lower than 2.19 dB (7.63 GHz) over the working frequency band.

Furthermore, the CP polarizer has been simulated at oblique incidences. In order to keep the electric field of the incident wave in the direction of the Y axis, we assume that the incidence is a

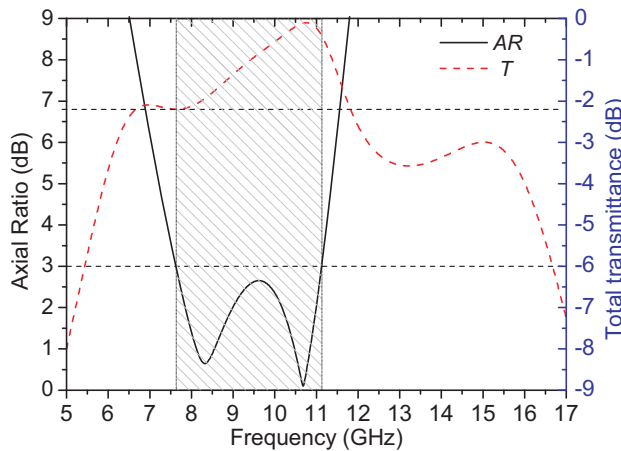


Figure 3. The total transmittance T and the axial ratio AR of the proposed polarizer at y -polarized normal incidence.

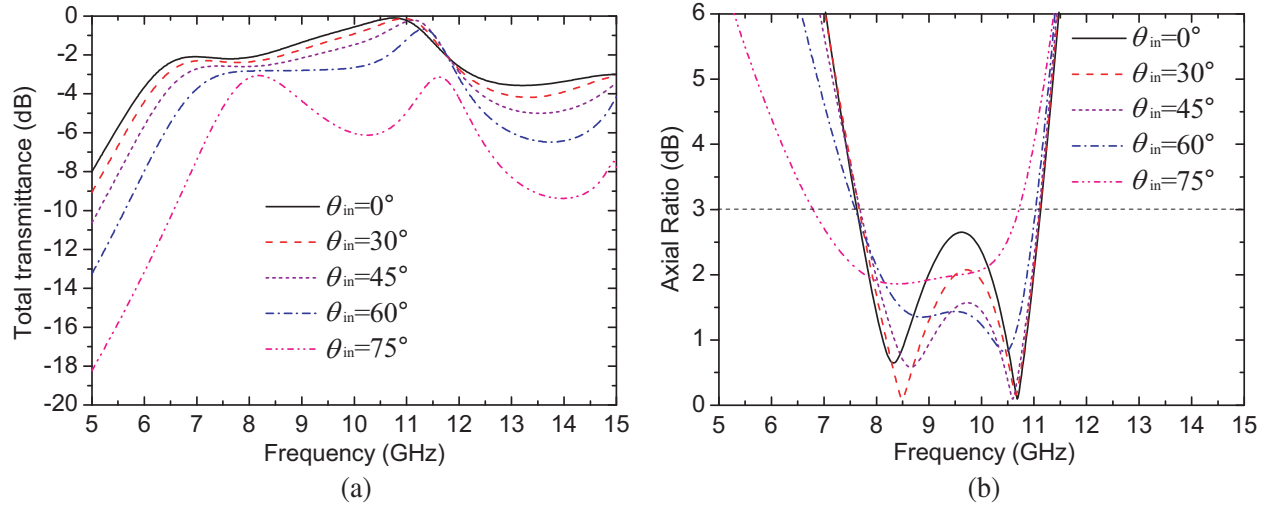


Figure 4. Simulated results of the proposed polarizer at oblique incidence: (a) The total transmittance T ; (b) The axial ratio AR .

TE wave in X - Z plane. When the incident angle θ_{in} was chosen as different values, the simulated results, shown in Fig. 4, indicate that the CP polarizer can maintain a stable polarization conversion performance under large-range incident angles. When the incident angle θ_{in} is less than 60° , the axial ratio AR continues to become smaller along with the increase of the incident angle, though the total transmittance T is decreased slightly. When the incident angle is equal to $\theta_{in} = 60^\circ$, the axial ratio AR can keep at less than 1.50 dB between 8.47 and 10.76 GHz. In addition, even if the incident angle is increased to $\theta_{in} = 75^\circ$, the axial ratio AR is still less than 3.00 dB between 6.79 and 10.71 GHz.

The above-mentioned results are all obtained at the y -polarized incidence. In fact, with the simulation using Ansoft HFSS we have obtained the transmission coefficients at x -polarized incidence at the same time, and concluded that the polarizer has no asymmetric transmission effect, and its reflection and transmission coefficients at the x - and y -polarized incidences are completely equal. It is just because the polarizer is based on the anisotropic metasurface, which is a symmetric structure with a pair of mutually perpendicular symmetric axes u and v along $\pm 45^\circ$ directions with respect to y -axis, as shown in Fig. 1(b). Especially the symmetric axes u is just the angle bisector of the right angle between the positive x - and y -axes, and this indicates that the x and y axes are completely symmetrical in the metasurface structure, so $t_{yy} = t_{xx}$, $t_{xy} = t_{yx}$, and the same LP-to-CP polarization conversion can be realized at x - and y -polarized incidences.

Furthermore, to get an insight into the cause of the LP-to-CP polarization conversion, we carry out another analysis in succession. Because the polarizer structure is symmetric with respect to both u and v axes, no cross-polarized component exists in the reflected and transmitted waves at u - and v -polarized incidences, and the transmission coefficients at the two incidences can be expressed as t_u and t_v , respectively. In addition, the u and v axes intersect with each other vertically, so t_u and t_v are mutually independent, and the total transmission performance of the polarizer can be completely determined by the two simple transmission coefficients. In fact, the above-assumed y -polarized incident wave can be decomposed into two equal u - and v -polarized components $E^i = E_0 e^{-jkz} \hat{e}_y = E_0 \cos(45^\circ) e^{-jkz} (\hat{e}_u + \hat{e}_v)$, so that by using the two transmission coefficients t_u and t_v can be obtained using the formula $E^t = E_0 \cos(45^\circ) e^{-jkz} (t_u \hat{e}_u + t_v \hat{e}_v)$. It is indicated that the polarization state of the transmitted wave can be determined by the difference between t_u and t_v . If the amplitudes of t_u and t_v are almost equal, and the phase difference $\Delta\varphi_{uv} = \arg(t_u) - \arg(t_v)$ between them is close to $\pm 90^\circ$, the transmitted wave will be converted to a CP one. To illustrate this, we have simulated the polarizer at u - and v -polarized incidences, and the simulated results, shown in Figs. 5(a) and (b), indicate that the magnitudes of t_u and t_v are almost equal, and the phase difference $\Delta\varphi_{uv}$ is close to -90° in the frequency range from 7.6 to 11.1 GHz, which implies that the two transmitted components at the two equal u - and v -polarized incidences will be combined into a circular polarized wave in this frequency band. Now the axial ratio

of the total transmitted wave can be calculated using the following formula

$$AR = \left(\frac{|t_u|^2 + |t_v|^2 + \sqrt{a}}{|t_u|^2 + |t_v|^2 - \sqrt{a}} \right)^{1/2} \quad (2)$$

wherein $a = |t_u|^4 + |t_v|^4 + 2|t_u|^2|t_v|^2 \cos(2\Delta\varphi_{uv})$. According to the simulated results in Figs. 5(a) and (b), the calculated AR is shown in Fig. 5(c), and it is indicated that the results obtained at the u - and v -polarized incidences are almost the same as those obtained at the y -polarized incidence.

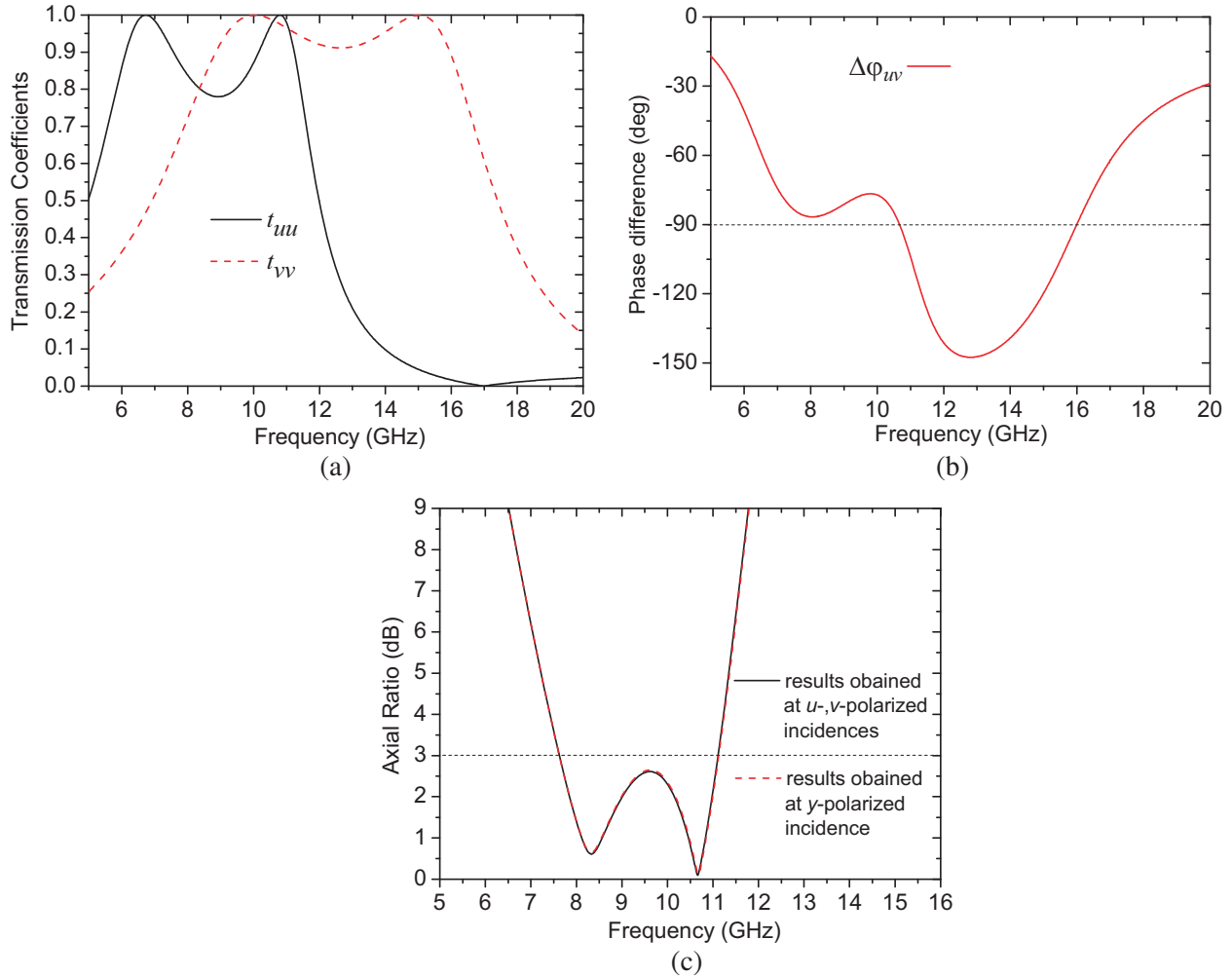


Figure 5. Simulated and calculated results of the proposed polarizer at u - and v -polarized incidences: (a) The magnitudes of t_{uu} and t_{vv} ; (b) The phase difference $\Delta\varphi_{uv}$; (c) The axial ratio AR .

From the above analysis, we can conclude that the orthotropy of the metasurface structure, which results in two independent transmission coefficients t_u and t_v , is the root cause of the polarization conversion, and the polarization state of the transmitted wave can be completely determined by the difference between t_u and t_v . When the amplitudes of t_u and t_v are almost equal, and the phase difference $\Delta\varphi_{uv}$ between them is close to $\pm 90^\circ$, the anticipated LP-to-CP polarization conversion can be realized at both x - and y -polarized incidences. However, for the proposed polarizer, why did these two points both happen in the frequency range from 7.6 to 11.1 GHz? In order to illustrate its physics mechanism, we have carried out an effective simulation at the frequency 10.81 GHz. As the simulated results, the surface currents on the top and bottom printed-metal-films at u - and v -polarized incidences

are presented in Figs. 6(a) and (b), respectively. It is indicated that these surface currents are both relatively large, which implies that a local electromagnetic resonance is caused at both u - and v -polarized incidences, so the magnitudes of t_u and t_v are both close to 1.0 at this frequency point, and they are almost equal in a finite frequency range (7.6–11.1 GHz). In addition, Fig. 6(a) shows that the directions of the surface currents on the top and bottom printed-metal-films are just opposite at the u -polarized incidence, which means that there is an inductive coupling between the top and bottom printed-metal-films, so the equivalent circuit model of the local electromagnetic resonance can be equivalent to an inductive coupled LC resonant circuit as shown in Fig. 6(c); however, in Fig. 6(b), it is indicated that the surface currents on the two-side printed-metal-films are in the same direction at the v -polarized incidence, and a capacitive coupling exists between the top and bottom printed-metal-films, so the equivalent circuit model of the local electromagnetic resonance shall be changed as a capacitive coupled LC resonant circuit in Fig. 6(d). In this way, the phase of t_v , which represents the amount of the phase lag of the transmitted wave relative to the incident wave, will be much larger than that of t_u . The phase difference $\Delta\varphi_{uv} = \arg(t_u) - \arg(t_v)$ will be a large negative number, and now it is just close to -90^{circ} in this frequency band (7.6–11.1 GHz) for these geometrical parameters of the unit cell are appropriate. Now both the points have happened, so the anticipated LP-to-CP polarization conversion has been realized.

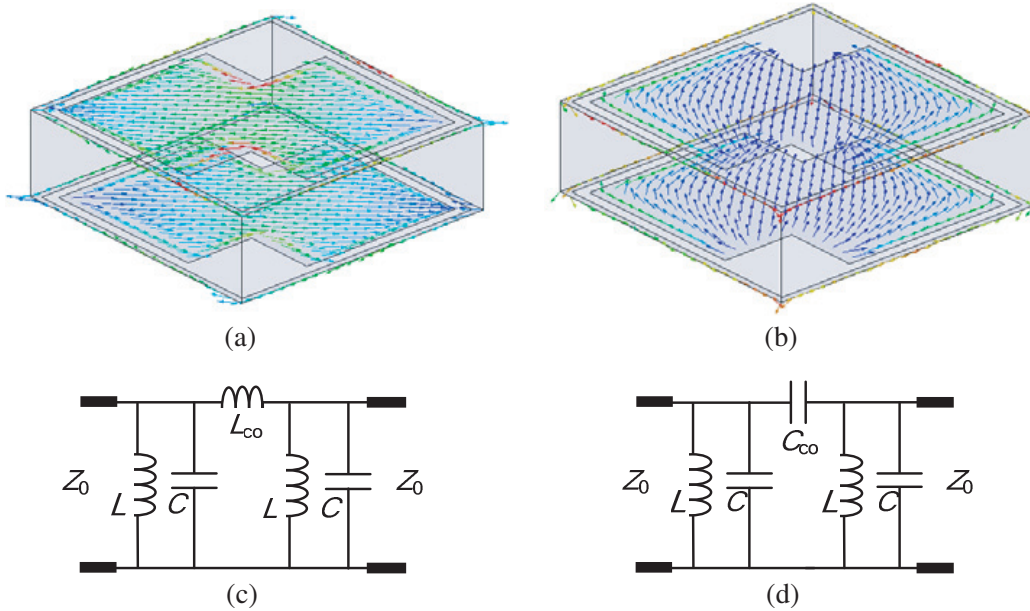


Figure 6. The surface current distributions, together with the equivalent circuit model, of the proposed polarizer at 10.81 GHz: (a) and (c) Those at u -polarized incidence; (b) and (d) Those at v -polarized incidence.

3. EXPERIMENTAL RESULTS

Finally, to realize an experimental validation for our design, a prototype of the proposed polarizer is fabricated using standard PCB etching techniques, which consists of 45×45 unit cells with an area of $360 \text{ mm} \times 360 \text{ mm}$ as shown in Fig. 7(a). We have carried out a detailed measurement on the experimental prototype in a microwave anechoic chamber, and the two transmission coefficients t_{yy} and t_{xy} at y -polarized normal incidence have been measured using a pair of transmitting and receiving horn antennas, which are connected to the two ports of a vector network analyzer (VNA). The axial ratio AR and the total transmittance T are obtained in succession using formula (1) and $T_{\text{all}} = |t_{yy}|^2 + |t_{xy}|^2$, respectively. The measured and simulated results are shown in Figs. 7(b) and (c), and it is indicated that the experiment results are basically in agreement with numerical predication.

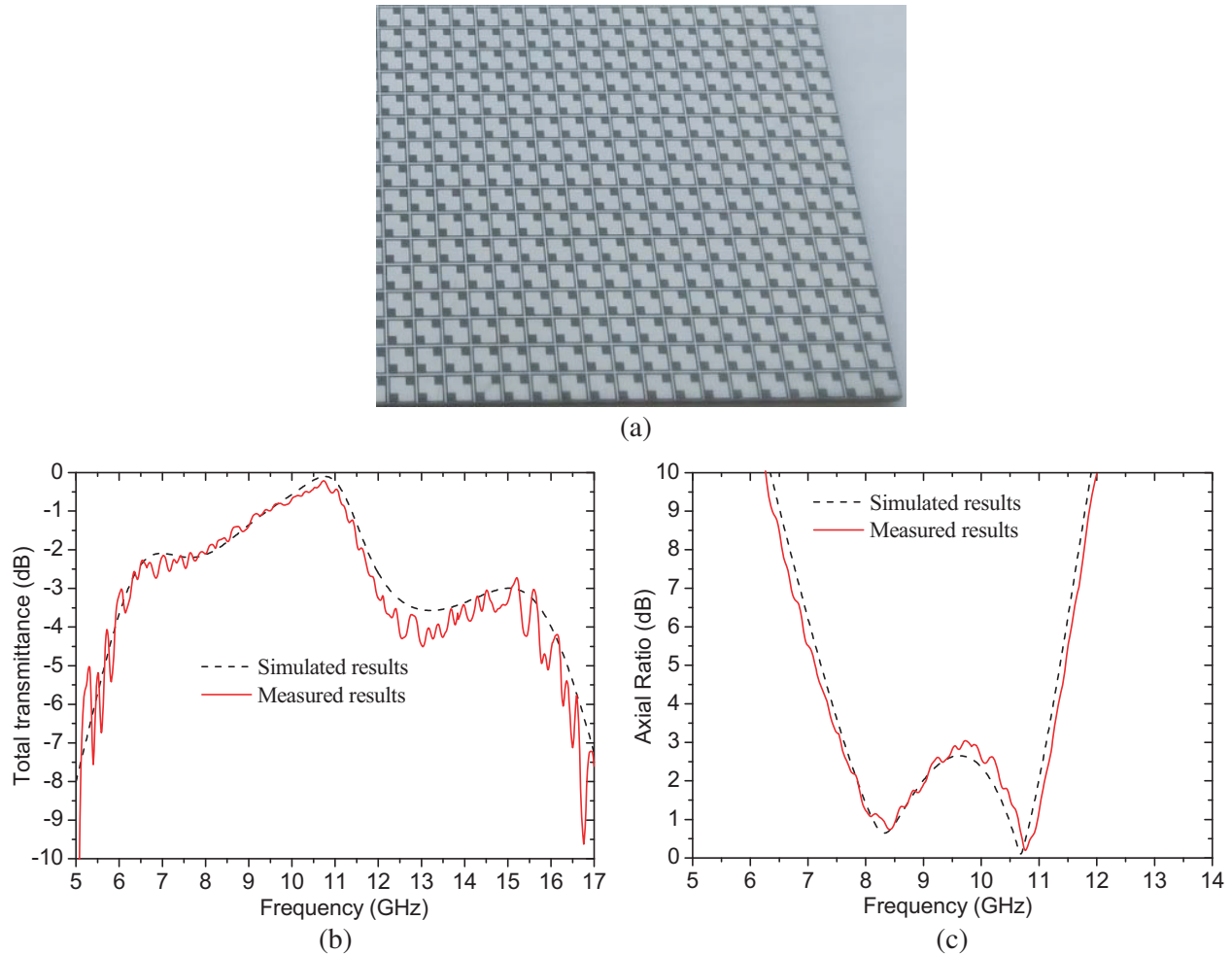


Figure 7. (a) The photograph of the fabricated prototype; (b) The comparison between the measured and simulated results of the total transmittance T and (c) the axial ratio AR .

4. CONCLUSION

In conclusion, a wide-angle and wide-band transmission-type circular polarizer is proposed in this work, which is based on a bi-layer anisotropic metasurface. Because it is an orthotropic structure with a pair of mutually perpendicular symmetric axes u and v along $\pm 45^\circ$ directions with respect to y -axis direction, at u -polarized and v -polarized incidences, it has two independent transmission coefficients t_u and t_v . The simulated results show that the amplitudes of t_u and t_v are basically equal, and the phase difference $\Delta\varphi_{vu}$ between them is close to -90° in the frequency range from 7.63 to 11.13 GHz, so the anticipated LP-to-CP polarization conversion can be realized in this frequency band at both x - and y -polarized incidences. Finally, one experiment is carried out, and the simulated and measured results are in agreement with each other. Compared to the previous designs, the proposed polarizer possesses a simpler geometry and greater stable performance under large incident angles, and at the same time, it has no asymmetric transmission effect, indicating that it may possess potential applications in polarization controlled devices, stealth surfaces, antennas, etc.

ACKNOWLEDGMENT

This work was supported by the National Natural Science Foundation of China (Grant No. 61471387), the research center for internet of things and big data technology of Xijing University.

REFERENCES

1. Kajiwara, A., "Line-of-sight indoor radio communication using circularly polarized waves," *IEEE Trans. Veh. Technol.*, Vol. 44, No. 3, 487–493, 1995.
2. Young, L., L. Robinson, and C. Hacking, "Meander-line polarizer," *IEEE Trans. Antennas and Propa.*, Vol. 21, No. 3, 376–378, 1973.
3. Huang, Y. H., Y. Zhou, and S. T. Wu, "Broadband circular polarizer using stacked chiral polymer films," *Optics Express*, Vol. 15, No. 10, 6414–6419, 2007.
4. Chen, H., J. Wang, and H. Ma, "Ultra-wideband polarization conversion metasurfaces based on multiple plasmon resonances," *Journal of Applied Physics*, Vol. 115, No. 15, 154504, 2014.
5. Gao, X., X. Han, and W. P. Cao, "Ultrawideband and high-efficiency linear polarization converter based on double V-shaped metasurface," *IEEE Transactions on Antennas & Propagation*, Vol. 63, No. 8, 3522–3530, 2015.
6. Sui, S., H. Ma, J. Wang, et al., "Symmetry-based coding method and synthesis topology optimization design of ultra-wideband polarization conversion metasurfaces," *Applied Physics Letters*, Vol. 109, No. 1, 063908, 2016.
7. Khan, M. I., Q. Fraz, and F. A. Tahir, "Ultra-wideband cross polarization conversion metasurface insensitive to incidence angle," *Journal of Applied Physics*, Vol. 121, No. 4, 045103, 2017.
8. Su, P., Y. Zhao, S. Jia, et al., "An ultra-wideband and polarization-independent metasurface for RCS reduction," *Scientific Reports*, Vol. 6, 20387, 2016.
9. Zhao, J. and Y. Cheng, "A high-efficiency and broad band reflective 90 linear polarization rotator based on anisotropic metamaterial," *Applied Physics B*, Vol. 122, No. 10, 255, 2016.
10. Cheng, Y. Z., C. Fang, X. S. Mao, R. Z. Gong, and L. Wu, "Design of an ultra-broad band and high-efficient reflective linear polarization convertor at optical frequency," *IEEE Photonics Journal*, Vol. 8, 7805509, 2016.
11. Sun, H., C. Gu, X. Chen, et al., "Ultra-wideband and broad-angle linear polarization conversion metasurface," *Journal of Applied Physics*, Vol. 121, No. 17, 1304–1404, 2017.
12. Zhao, J. C. and Y. Z. Cheng, "Ultra-broad band and high-efficiency reflective linear polarization convertor based on planar anisotropic metamaterial in microwave region," *Optik — International Journal for Light and Electron Optics*, Vol. 136, 52–57, 2017.
13. Fang, C., Y. Cheng, Z. He, J. Zhao, and R. Gong, "Design of a wideband reflective linear polarization converter based on the ladder-shaped structure metasurface," *Optik — International Journal for Light and Electron Optics*, Vol. 137, 148–155, 2017.
14. Xu, P., S. Y. Wang, and G. Wen, "A linear polarization converter with near unity efficiency in microwave regime," *Journal of Applied Physics*, Vol. 121, No. 14, 1804–1949, 2017.
15. Xu, K. K., Z. Y. Xiao, and J. Y. Tang, "Ultra-broad band and dual-band highly efficient polarization conversion based on the three-layered chiral structure," *Physica E*, Vol. 81, 169–176, 2016.
16. Zhou, G., X. Tao, Z. Shen, et al., "Designing perfect linear polarization converters using perfect electric and magnetic conducting surfaces," *Scientific Reports*, Vol. 6, 38925, 2016.
17. Huang, C., Y. Feng, J. Zhao, et al., "Asymmetric electromagnetic wave transmission of linear polarization via polarization conversion through chiral metamaterial structures," *Physical Review B*, Vol. 85, No. 19, 195131, 2012.
18. Huang, X., D. Yang, S. Yu, et al., "Dual-band asymmetric transmission of linearly polarized wave using II-shaped metamaterial," *Applied Physics B*, Vol. 117, No. 2, 633–638, 2014.
19. Xu, Y., Q. Shi, Z. Zhu, et al., "Mutual conversion and asymmetric transmission of linearly polarized light in bilayered chiral metamaterial," *Optics Express*, Vol. 22, No. 21, 25679, 2014.
20. Liu, D., Z. Xiao, X. Ma, et al., "Dual-band asymmetric transmission of chiral metamaterial based on complementary U-shaped structure," *Applied Physics A*, Vol. 118, No. 3, 787–791, 2015.
21. Fang, S., K. Luan, H. F. Ma, et al., "Asymmetric transmission of linearly polarized waves in terahertz chiral metamaterials," *Journal of Applied Physics*, Vol. 121, No. 3, 033103, 2017.

22. Cheng, Y., R. Gong, and L. Wu, "Ultra-broad band linear polarization conversion via diode-like asymmetric transmission with composite metamaterial for terahertz waves," *Plasmonics*, Vol. 12, No. 4, 1113–1120, 2017.
23. Dou, T., L. Wei, X. Ran, et al., "Broadband asymmetric transmission of linearly polarised wave based on bilayered chiral metamaterial," *IET Microwaves Antennas & Propagation*, Vol. 11, No. 2, 171–176, 2017.
24. Kuwata-Gonokami, M., N. Saito, Y. Ino, et al., "Giant optical activity in quasi-two-dimensional planar nanostructures," *Phys. Rev. Lett.*, Vol. 95, No. 22, 227401, 2005.
25. Yan, S. and G. A. E. Vandenbosch, "Compact circular polarizer based on chiral twisted double split-ring resonator," *Appl. Phys. Lett.*, Vol. 102, No. 10, 103503–103504, 2013.
26. Martinez-Lopez, L., J. Rodriguez-Cuevas, J. I. Martinez-Lopez, and A. E. Martynyuk, "A multilayer circular polarizer based on bisected split-ring frequency selective surfaces," *IEEE Antennas & Wireless Propagation Letters*, Vol. 13, No. 2, 153–156, 2014.
27. Pfeiffer, C., C. Zhang, V. Ray, et al., "High performance bianisotropic metasurfaces: Asymmetric transmission of light," *Physical Review Letters*, Vol. 113, No. 2, 023902, 2014.
28. Cheng, Y., C. Wu, Z. Z. Cheng, and R. Z. Gong, "Ultra-compact multi-band chiral metamaterial circular polarizer based on triple twisted split-ring resonator," *Progress In Electromagnetics Research*, Vol. 155, 105–113, 2016.
29. Liu, Y., Y. Luo, et al., "Linear polarization to left/right-handed circular polarization conversion using ultrathin planar chiral metamaterials," *Applied Physics A*, Vol. 123, No. 9, 571, 2017.
30. Baena, J. D., et al., "Broadband and thin linear-to-circular polarizers based on self-complementary zigzag metasurfaces," *IEEE Trans. Antennas Propag.*, Vol. 65, No. 8, 4124–4133, 2017.
31. Gansel, J. K., M. Thiel, M. S. Rill, et al., "Gold helix photonic metamaterial as broadband circular polarizer," *Science*, Vol. 325, No. 5947, 1513, 2009.
32. Gansel, J. K., M. Latzel, et al., "Tapered gold-helix metamaterials as improved circular polarizers," *Appl. Phys. Lett.*, Vol. 100, No. 10, 101109–101109-3, 2012.
33. Kaschke, J., L. Blume, et al., "Metamaterial for broadband circular polarization conversion," *Advanced Optical Materials*, Vol. 3, No. 11, 1411–1417, 2015.
34. Chen, M., L. J. Jiang, W. Sha, et al., "Polarization control by using anisotropic 3-D chiral structures," *IEEE Trans. Antennas Propag.*, Vol. 64, No. 11, 4687–4694, 2016.
35. Ji, R., S. W. Wang, X. Liu, X. Chen, and W. Lu, "Broadband circular polarizers constructed using helix-like chiral metamaterials," *Nanoscale*, Vol. 8, No. 31, 14725–14729, 2016.